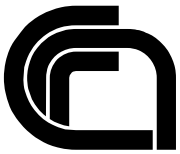

Consiglio Nazionale delle Ricerche

A Measurement-based Study of Beaconing Performance in IEEE 802.11p Vehicular Networks

F. Martelli, M. Elena Renda, G. Resta, P. Santi

IIT TR-16/2011

Technical report

Luglio 2011

Istituto di Informatica e Telematica

A Measurement-based Study of Beaconing Performance in IEEE 802.11p Vehicular Networks

Francesca Martelli, M. Elena Renda, Giovanni Resta, and Paolo Santi
IIT - CNR, Pisa – Italy

***Abstract*—Active safety applications for vehicular networks aims at improving safety conditions on the road by raising the level of "situation awareness" onboard vehicles. Situation awareness is achieved through exchange of beacons reporting positional and kinematic data. Two important performance parameters influence the level of situation awareness available to the active safety application: the *beacon (packet) delivery rate* (PDR), and the *packet inter-reception* (PIR) time. While measurement-based evaluations of the former metric recently appeared in the literature, the latter metric has not been studied so far. In this paper, for the first time, we estimate the PIR time and its correlation with PDR and other environmental parameters through an extensive measurement campaign based on IEEE 802.11p technology.**

Our study discloses several interesting insights on PIR times that can be expected in a real-world scenarios, which should be carefully considered by the active safety application designers. A major insight is that *the packet inter reception time distribution is a power-law* and that *long situation awareness black-outs are likely to occur in batch*, implying that situation awareness can be severely impaired even when the average beacon delivery rate is relatively high. Furthermore, our analysis shows that *PIR and PDR are only loosely (negatively) correlated*, and that *the PIR time is almost independent of speed and distance between vehicles*.

A third major contribution of this paper is promoting the Gilbert-Elliot model, previously proposed to model bit error bursts in packet switched networks, as a very accurate model of beacon reception behavior observed in real-world data.

I. Introduction

Vehicular networks are considered a very promising technology to improve safety conditions on the road. Active safety applications are a class of applications enabled by short range vehicular radio communications aimed at raising the level of a driver's "situation awareness", with a substantial benefit in terms of improved safety conditions and better traffic efficiency. Among active safety applications, we mention electronic emergency braking light, lane change assistant, lane merging assistant, intersection collision warning, etc. [15].

The successful realization of active safety applications poses hard challenges to the underlying communication technology, which should enable fast and reliable exchange of information between neighboring vehicles in an environment characterized by high mobility and typically harsh radio propagation conditions. The Dedicated Short Range Communication (DSRC) initiative [11] is aimed at defining standards at various levels of the network architecture to realize such dependable short-range radio technology for vehicular communications. In particular, the recently released IEEE 802.11p standard amends the well-known 802.11 protocol suite with the goal of improving quality in vehicular communications. The standard operates in the 5.9 GHz frequency band, and provides data rates between 3 and 27 Mbps.

The fundamental mechanism underlying active safety applications is *beaconing*, through which applications running onboard vehicles become aware of the position and status of surrounding vehicles. Beaconing consists in the periodic, single-hop broadcast transmission of status messages – called *beacons* – containing vehicle positional and kinematic data. Thus, understanding beaconing performance is a fundamental step in the process of designing active safety applications. This explains the considerable attention that the vehicular networking community has devoted to the study and optimization of beaconing [1], [5], [9], [10], [13], [14]. In particular, two parameters have been identified as the most relevant to characterize beaconing performance: the *beacon delivery rate* and *beacon inter-reception time*.

Beacon delivery rate refers to the fraction of correctly received beacons over the total number of transmitted beacons, i.e., it is equivalent to the well-known packet delivery rate (PDR) metric. Beacon (packet) inter-reception time (PIR), first defined in [5], is defined as the interval of time elapsed between two successful beacon receptions. To understand why both PDR and PIR are important in characterizing situation awareness, consider the two following scenarios. In both scenarios, 50% of the beacons transmitted by vehicle A with a 10Hz frequency in an interval of 10 sec are received at vehicle B, i.e., vehicle B receives 50 beacons in both cases. However, the reception pattern is very different. In scenario 1, beacons are received in an alternate fashion: the first beacon is received, the second is missed, the third is received, and so on. In scenario 2, beacons are received in batch: 25 beacons are received in the first two seconds of the interval, then no beacon is received for 5 seconds, and the remaining 25 beacons are received in the last three seconds of the interval. Clearly, scenario 1 and 2 are very different from the situation awareness viewpoint: in the former case, vehicle B's knowledge of vehicle A's position and status is outdated of at most 200 msec; in the latter case, there is a situation awareness blackout of at least 5 sec. Considering that a vehicle can move of more than one hundred meters in 5 sec at highway speeds, it is clear that situation awareness is severely impaired in scenario 2, resulting in possibly undetected dangerous situations.

So far, beaconing performance has been mostly studied through analysis and simulation, and only very recently a few papers evaluated PDR based on on-the-field measurements –

see Section II. However, as commented above PDR alone is not sufficient to fully understand the level of situation awareness available to active safety applications. Thus, ours can be considered as the *first study of practical beaconing performance* – including both PDR and PIR – based on an extensive set of *on-the-field measurements obtained in normal traffic conditions*.

Our measurement-based characterization of beaconing performance discloses several interesting insights:

- the *PIR time distribution is heavy-tailed*. More specifically, it is a power law of relatively low exponent. Furthermore, relatively long situation awareness blackouts are likely to occur in batch. These facts have important implications on active safety application design, which shall be able to cope with relatively long and repeated situation awareness blackouts;
- *PIR and PDR are loosely correlated metrics*, promoting PIR time as the most important metric for estimating the degree of "situation awareness" in vehicular networks.

Another major contribution of this paper is promoting the Gilbert-Elliot model [6], [8] as a very accurate vehicular link channel model: in the last part of the paper, we show that this model, which we rename L/N model in the context of vehicular networks to emphasize effect of LineOfSight (LOS)/NonLineOfSight (NLOS) conditions on link quality, can be tuned to almost perfectly resemble the beacon reception patterns observed in our collected measurements. Given its simplicity and analytical tractability, we then propose the L/N model as an invaluable tool in the design and analysis of active safety applications.

II. Related Work

Given its importance within the realm of active safety applications, beaconing performance characterization and optimization has been subject of intensive research in recent years. Most studies are based on analysis and simulation, and are typically aimed at understanding and optimizing the communication parameters (data rate, transmission power, etc.) [10], [14]. In [13], the authors analyze multi-hop information propagation using a simple link model, corresponding to the geometric link model that we will consider in the last part of this paper. Other studies consider specific active safety applications, such as cooperative collision warning [5], [16].

Only very recently some papers have been published reporting results from on-the-field experiments using IEEE 802.11p compliant radios. Here, we discuss only results relevant to the beaconing application considered in this paper, and we do not consider the several experimental works aimed at evaluating PHY layer features of the vehicular radio link (see, e.g., [2] and references therein).

To our best knowledge, all existing measurement-based studies focus on PDR [1], [9] or on application-layer goodput [12], and only some of them [1], [9] consider vehicle-to-vehicle communications.

In [9], the authors consider an intersection collision warning application, and evaluate PDR and RSSI as a function of the distance of the two vehicles from the intersection. The authors consider different transmit power values in their study, and conclude that intermediate power levels can provide good performance while at the same time reducing congestion in the wireless channel.

In [1], the authors present an extensive analysis of PDR in different scenarios for what concerns propagation environment, data rate, etc. The authors also analyze temporal, spatial, and symmetric correlation of PDR values, and conclude that, while temporal and spatial correlation are weak, symmetric correlation is instead quite strong.

To our best knowledge, none of the existing measurement-based studies addresses the problem of characterizing the PIR time distribution, and its relationship with PDR and other environmental factors such as speed and distance between vehicles. As we have exemplified in the previous section, beacon delivery rate alone is not sufficient to quantify the level of situation awareness delivered to the active safety application. More information about the temporal pattern of successful beacon receptions is needed for this purpose, which motivated the authors of [5] to introduce the notion of packet inter-reception time.

III. Experiments Setup

A. Hardware

Experiments have been performed using two IEEE 802.11p compliant devices, namely the LinkBird-MX v3 units produced by NEC. The LinkBird-MX units are embedded Linux machines (kernel 2.6.19) based on a 64 bits MIPS processor working at 266Mhz. The characteristics of LinkBird-MX 802.11p network interface are reported in Table I.

LinkBird-MX units were connected to a small-size, omnidirectional WiMo antenna, whose characteristics and form factor fit well with vehicular applications. The antenna operates at 5.5–5.8GHz frequency range, has $5dBi$ gain, and is 108 mm long. The antennas were mounted on the roof of the vehicles for performing vehicle-to-vehicle radio measurements. The onboard equipment on each vehicle is composed of a LinkBird-MX unit, a GPS receiver, a laptop, and a rooftop antenna.

Parameter	Details
Frequency/Channel	$5725 - 5925$ MHz
Bandwidth	$10 - 20$ MHz
Version	IEEE802.11p Draft 3.0, July 2007
Transmit Power	Max 21 dBm (Europe)
Bitrates (10MHz)	$3, 4.5, 6, 9, 12, 18, 24, 27$ Mbps
Bitrates (20MHz)	$6, 9, 12, 18, 24, 36, 48, 54$ Mbps

TABLE I
Characteristics of LinkBird-MX 802.11p network interface.

Several radio channels in the 5.9GHz frequency band have been reserved for vehicular systems both in Europe and US. Among these channels, one is reserved for safety applications only (the *control channel*). Given our focus on measuring performance of beaconing, which is at the basis of active safety applications, we used the control channel – in Europe, channel 180 at 5.9 GHz – for all our measurements.

B. Beaconing application

We developed a simple beaconing application, which sends packets – henceforth called *beacons* – at a regular interval. The beaconing interval has been set to 100 ms, according to recommendations for active safety applications [11].

Beacons are generated by the application running on the laptop, sent to the LinkBird-MX unit through an Ethernet link, and then transmitted on air using the single-hop broadcast primitive provided by the LinkBird-MX protocol stack – called C2X stack. A packet sent in single-hop broadcast is received by all the nodes within the transmitter's communication range.

A beacon contains the following information: the vehicle ID, the packet ID (increased by one at each transmission), the vehicle latitude, longitude, speed, heading, and current time (all taken from GPS receiver). Each beacon has a 100 bytes payload, which is considered to be a typical size for active safety applications [11] – without security overhead. In fact, beacons are envisioned to carry not only GPS data, but also data collected from various onboard sensors reporting, e.g., steering wheel angle, braking system status, vehicle size, etc. Since we do not have direct access to these data in our experiments, we use a padding of 73 bytes to generate a 100 bytes beacon.

Beacons are transmitted at full power (21 dBm in Europe) using the lowest coding rate (1/2) with BPSK modulation, corresponding to a PHY layer raw data rate of $6Mbps$ with $20Mhz$ channel bandwidth, in agreement with latest recommendations [7], [10]. Usage of the lowest available data rates is mandatory for active safety applications, due to the typical usage of single-hop broadcast packets (which can be sent only at the lowest data rate), and to the better communication reliability provided by the lowest data rate.

The beaconing application also generates data traces as follows. The application records both transmission and reception events: for each transmitted beacon, the application running on vehicle A records the vehicle ID, the packet ID, and A's GPS data (latitude, longitude, speed, and heading), thus mirroring the information contained in the transmitted beacon. Also, whenever the application running on vehicle A receives a beacon from another vehicle B, it stores the following information: the beacon content – B's vehicle ID, packet ID, and B's GPS data –, the own GPS data (latitude, longitude, speed, heading and time), and the current system time. Note that the recorded system time at A is not necessarily synchronized with GPS time, nor with the system time at B. However, synchronization is not needed here, as the sole purpose of recording system time of a reception event is allowing an accurate measurement of the PIR time: with system time, we are able to measure PIR time with a $1ms$ accuracy. On the other hand, the GPS receivers used in our experiments provide time readings with a $1s$ accuracy, which is insufficient for accurately measuring PIR time – but sufficient (with some trick) to allow temporal alignment of the recorded traces.

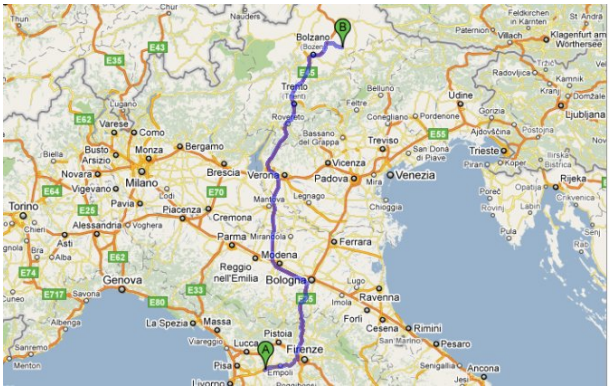

Fig. 1. Map reporting the return trip from Montopoli Valdarno to S.Cristina Valgardena.

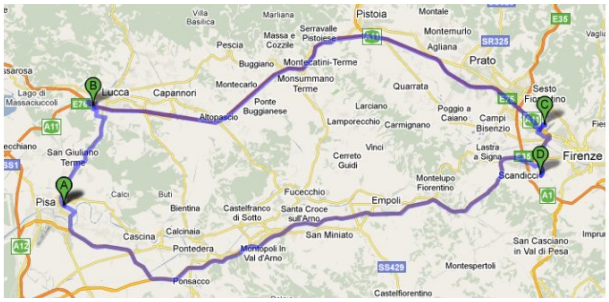

Fig. 2. Map reporting the return trip from Pisa to Florence.

IV. Measurements

A. Data collection

Measurements were collected during several data collection campaigns performed in the months of January and February 2011. The first two sets of measurements were taken during a two-way trip from Montopoli Valdarno to S. Cristina Valgardena, Italy (see Figure 1). The one way trip from Montopoli to S. Cristina is 453 Km long. A second group of measurements were taken during two two-way trips from Pisa to Florence – see Figure 2 – where each two-way trip is about 176 Km. Overall, measurements were taken along a total of 1260 Km per vehicle, comprised of about 1151 Km of highways, 82 Km of suburban road, and 27Km of urban road. Indeed, the total amount of traveled kilometers during measurement campaigns amounts to 2520 Km, as two vehicles have been used to both transmit and receive beacons.

B. Data post-processing

The raw traces generated during the measurement campaigns have been post-processed to generate data that can be directly used to evaluate beaconing performance.

The first problem we addressed was temporal alignment of the four sets of traces generated for each leg of a trip. The transmit traces generated by the two vehicles have been used for this purpose. Traces have been aligned using the GPS time reading. We recall that our GPS devices provide time reading with a $1s$ granularity, which is insufficient for accurate temporal alignment of data traces considering that a vehicle can move of more than $30m$ in a second in a highway. However, the GPS device is polled with a 10Hz frequency

(the beaconing frequency), thus allowing temporal alignment of transmit traces with an accuracy of about $0.1s$, which we deem sufficient for our purposes (considering also the inherent inaccuracy in GPS positional data). Temporal alignment of the transmit traces allows computing the distance between vehicles during the trip.

Note that GPS position readings might be invalid for relatively long periods of time due to, e.g., galleries, reduced number of visible satellites, and so on. This implies that valid GPS readings of *both* vehicles have been recorded only for a portion of a trip. We define a GPS position reading taken at time t to be *valid* if and only if:

a) it has been updated with respect to the previous reading taken at time $t-1$;

b) the distance between the position of the vehicle at time t and $t-1$ is compatible with the GPS speed reading, i.e.

$$d(t-1,t) \leq 1.5 \cdot v_{max} \ ,$$

where $d(t-1,t)$ is the distance between vehicle position at time t and that at time $t-1$, and v_{max} is the largest speed reading returned by GPS at times $t-1$ and t.

Criterion b) has been introduced to filter out situations in which a sudden change in environmental conditions (e.g., new satellites becoming visible) resulted in very different consecutive GPS position readings.

Once transmit traces have been temporally aligned, *valid segments* of a trip have been identified, where a valid segment is defined as a portion of a trip during which the GPS position readings of *both* vehicle A and B are continuously valid for a time interval of at least $30s$. Intuitively, a valid segment defines a portion of a trip for which the position of both vehicles can be accurately estimated. Thus, each trip is broken down into a number of valid segments. Beaconing performance estimation reported in the remainder of this paper will be based only on the analysis of traces collected in valid segments of the various trips, which amount to about 925 Km overall.

V. Aggregate PIR Time Distribution

Which is the PIR time distribution? A first observation that we derived from the extensive amount of collected data (over $448K$ transmission events and over $275K$ reception events have been recorded) is that the PIR time can be considered, for all practical purposes, as a *discrete* random variable[1]. In fact, PIR values computed from the receiver traces always matched almost perfectly with a value of the form $k \cdot T$, where $k \geq 1$ is an integer and T is the beaconing period of 100 ms. Thus, random variable PIR denoting the time elapsing between two successive successful beacon receptions can be modeled as $PIR = k \cdot T$, where T is a constant corresponding to the beaconing period, and k is a random integer denoting the number of periods elapsed between two successful receptions.

In order to characterize PIR time distribution, we observe that a sound notion of PIR time requires the two vehicles

[1]This observation applies to the low channel load scenarios considered in our measurements campaign.

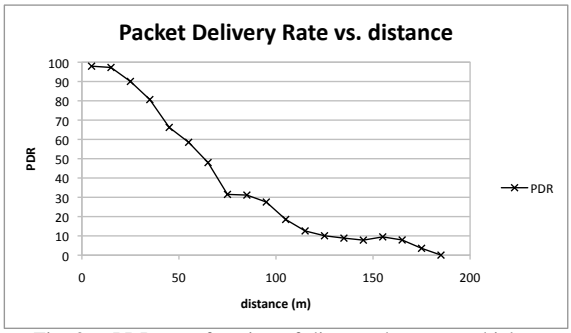

Fig. 3. PDR as a function of distance between vehicles.

to remain within each other transmission range during the timespan between successive successful beacon receptions. In fact, the aim of the PIR metric is to quantify the degree of "situation awareness" achieved when two vehicles are within each other transmission range. Clearly, there can be no situation awareness if two vehicles are not able to communicate.

Given the above observation, before proceeding further we need to define a notion of transmission range, that can be used to filter out portion of the data traces during which vehicles were not continuously within each other transmission range.

To characterize the transmission range, we analyze the dependence between PDR and distance between vehicles (see Figure 3). It is interesting to note that there are two relatively flat regions in the PDR vs distance curve: one in the range of distances between 70 m and 100 m, where PDR is about 30%; and one in the range of distance between 110 m and 170 m, where the PDR is about 10%. These flat regions can be used to define a notion of transmission range, i.e., of a distance up to which beacons can be received with a given minimum reliability. More specifically, in the following we define a *strict* and *loose* notion of transmission range, with the *strict* transmission range corresponding to 80 m, and the *loose* transmission range corresponding to 160 m.

It is interesting to compare the two values of transmission range defined above with those reported in the literature. In [1], the authors evaluate the PDR vs. distance function using extensive measurements in different vehicular scenarios. For all the scenarios considered, the reported transmission ranges are higher than the ones resulting from our studies. For instance, according to [1], we have a PDR of about 0.4 at 450 m. A possible reason explaining this difference in measured transmission ranges could be related to the hardware used in the experiments. In fact, while our NEC LinkBird-MX radios fullfil the requirements for minimum radio sensitivity dictated by DSRC, according to which sensitivity must be -85dBm at 3Mbs [4], in [1] the authors use radios with a much lower sensitivity of -94dBm. Thus, much longer transmission ranges can be in principle achieved using the radios of [1] given the same intensity of the received signal.

The PIR time distributions for strict and loose transmission range resulting from filtering out irrelevant portions of the data traces are reported in Figure 4. More specifically, the figure reports the complementary cumulative density function (ccdf) of random variable PIR, i.e., $P(PIR > k)$. The mean value of the PIR random variable is 126.29 msec with strict

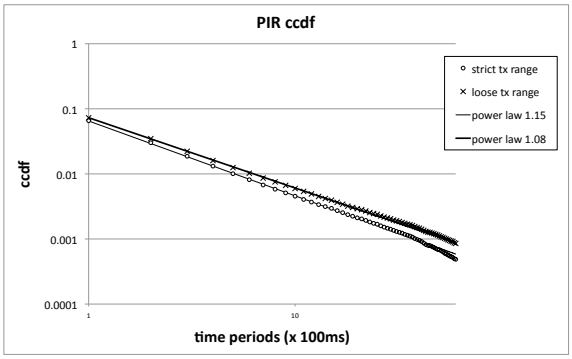

Fig. 4. PIR time ccdf and power law fitting (axes are in log scale).

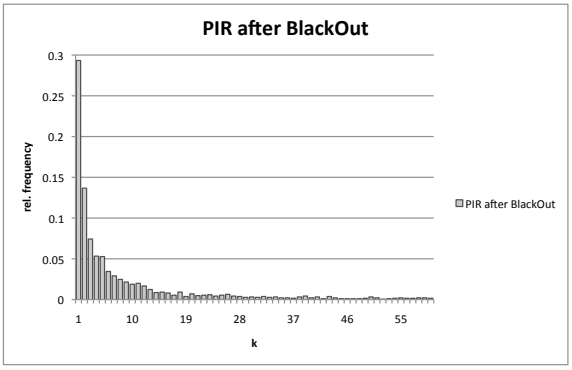

Fig. 5. Probability mass function of the PIR distribution after a blackout.

transmission range, and 134.92 msec with loose transmission range. The median is 100 msec in both cases. Indeed, the PIR distribution is highly concentrated on the first term: event $(PIR = 1)$ has relative frequency 0.9344 with strict transmission range, and 0.9277 with loose transmission range. The remaining probability mass, though, is well spread among the larger terms. In fact, independently of the definition of transmission range, the PIR time ccdf is linear in log-log scale, i.e., *it is a power law*. Indeed, the following power laws almost perfectly fit experimental data:

$$P(PIR > k) = 0.065 \cdot \left(\frac{1}{k}\right)^{1.15} \quad \text{for strict tx range ,}$$

and

$$P(PIR > k) = 0.073 \cdot \left(\frac{1}{k}\right)^{1.08} \quad \text{for loose tx range ,}$$

What are the implications of the power law trend of PIR time? The most important implication of the power law trend is that *the PIR time distribution is heavy tailed*: the probability of having relatively long PIR time is relatively high. The above observation applies to both definitions of transmission range: not only the PIR time is a power law in both cases, but the exponent of the power law is indeed very similar.

A consequence of the observed power law trend is that, when designing active safety applications, relatively long periods of time during which situation-awareness is impaired should be expected. For instance, the probability that the PIR time exceeds 1 sec – call this event a *blackout* – is about 0.006 with loose transmission range, which is apparently a low value. However, we have to consider that the PIR time value is sampled very frequently: on the average, a new PIR value is generated every 134.92 msec (loose tx range). Considering a blackout as a Bernoulli event with success probability 0.006, and assuming independence of blackouts[2], we have that blackouts on the average occur once every 1/0.006 samples, i.e., once every 22.5 sec. Thus, we can expect a situation-awareness black-out of at least 1 sec once every 22.5 sec on average. Considering that a vehicle can easily travel for 30-40 m in a highway scenario during one sec, it is evident that potentially dangerous situations might remain undetected during blackouts.

A third implication of the power law trend is related to modeling of the wireless link between vehicles, and is carefully investigated in Section VII: as we shall see, the fact that the PIR time distribution has a fat tail is a clear evidence of the fact that the simple wireless link model often used in vehicular network analysis [13], [16], according to which a packet is successfully received within transmission range with a fixed probability $0 < p \leq 1$, does not reflect packet reception behaviors observed in real world.

Are blackouts isolated? To answer this question, we have evaluated the distribution of the first PIR event after a blackout occurs in case of loose transmission range. More formally, we have evaluated the probability mass function of the event $(PIR_t = k | PIR_{t-1} > 10)$, where PIR_i is the i-th packet inter-reception time observation. The rationale for this investigation is the following: if blackouts were temporally independent events, the shape of the conditioned PIR distribution would be very similar to the shape of the unconditioned PIR distribution. Otherwise, positive or negative temporal correlation of blackouts is displayed.

The PIR time distribution observed after a blackout is reported in Figure 5. The shape of the distribution is considerably different from that of the unconditioned PIR time distribution (see also Figure 10 later on in the paper): the probability mass of the first event is 0.2933, as compared to 0.9277 in the unconditioned distribution; the mean and median are 1.384 sec and 250 msec, as compared to 134.9 msec and 100 msec in the unconditioned distribution. In general, the probability mass is shifted towards larger terms (heavier tail) in the conditioned distribution. For instance, the probability of having a blackout, which is 0.006 in the unconditioned distribution, is 0.261 after conditioning, i.e., more than 44 times larger. This clearly indicates a strong positive temporal correlation between blackout events: the fact that a blackout is just occurred considerably increases the probability of observing another blackout in the next sample. Thus, *blackout events are likely to occur in batch*, further challenging the design of effective active safety applications.

As we will see in Section VII, blackout temporal correlation can be explained by the L/N vehicular link model: if a blackout occurred, it is likely that the link between the two vehicles is in

[2]In the following, we show that blackouts are not independent events. Independency is assumed here for the purpose of back-of-the-envelope calculations only.

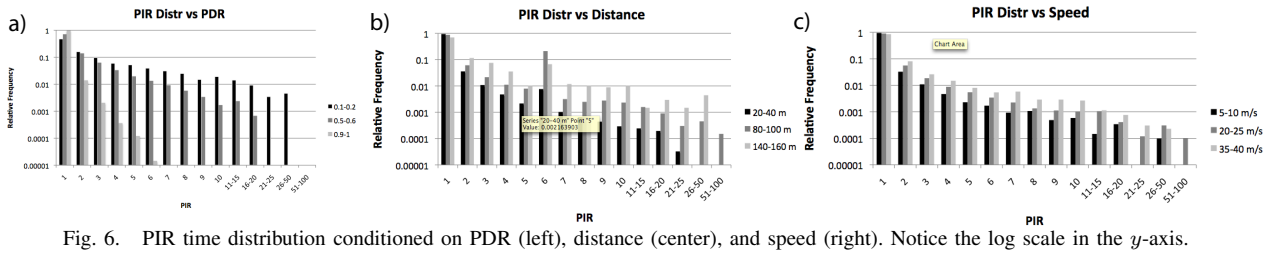

Fig. 6. PIR time distribution conditioned on PDR (left), distance (center), and speed (right). Notice the log scale in the y-axis.

NLOS conditions; if NLOS conditions are relatively persistent, it is then very likely that also the next observed PIR time will be relatively long.

VI. Conditioned PIR Time Distributions

Is the PIR time distribution correlated to PDR? To answer this question, we have computed the Pearson correlation coefficient[3] between PIR time measurement and the PDR observed in the 5 seconds preceding a successful reception event (which corresponds to a PIR time measurement). As seen from Table II, the coefficient reveals a weak inverse correlation between PIR and PDR. Thus, PDR values cannot be directly used to estimate PIR time. Since relevant PIR events from the "situation-awareness" viewpoint are those corresponding to relatively large PIR values (say, PIR times $\geq 1sec$), we have computed the correlation coefficient also on the restricted data set formed of the (PIR, PDR) pairs with $PIR \geq 10$. As seen from Table II, also in this case correlation is weak, although somewhat stronger than in case the entire data set is considered. The weak negative correlation between PIR time and PDR can be noticed also in Figure 6-a), reporting the PIR time distribution conditioned on different ranges of observed PDR values: as seen from the figure, higher PDR values tend to reduce the tail of the PIR time distribution.

PIR vs.	**All data set**	$PIR \geq 10$
PDR	-0.2313	-0.3543
distance	0.0856	0.1458
speed	0.0423	0.1084

TABLE II
Correlation coefficients between PIR time and PDR, distance, and speed.

Is the PIR time distribution correlated to distance? To answer this question, we have computed the correlation coefficient between the PIR time and the average distance between vehicles in the time interval elapsing between consecutive successful beacon receptions. The result, reported in Table II, shows a negligible correlation between distance and PIR time, which is confirmed also by the PIR time distributions conditioned on different distance values reported in Figure 6-b). Also when restricted to PIR values ≥ 10, the correlation between distance and PIR time remains barely noticeable (see Table II).

Is the PIR time distribution correlated to speed? To answer this question, we have computed the correlation coefficient between the PIR time and the average speed of vehicles in the time interval elapsing between consecutive successful beacon receptions. The result, reported in Table II, shows a negligible correlation between speed and PIR time, which is confirmed also by the PIR time distributions conditioned on different speed values reported in Figure 6-c). Also when restricted to PIR values ≥ 10, the correlation between speed and PIR time remains negligible (see Table II).

[3]We recall that the Pearson correlation coefficient takes values in $[-1, 1]$, with -1 and 1 representing maximal correlation (negative and positive, respectively), and 0 representing no correlation.

VII. Vehicular link models

Can a simple vehicular link model resembling observed PIR time distribution be defined? To answer this question, in this section we consider three candidate models, which we briefly introduce below. These models are aimed at modeling a situation in which the two vehicles are within each other transmission range, where the transmission range can be thought of as a value empirically defined as in Section V. For simplicity, and in accordance to the observation in Section V, in all models we assume time is discretized into 100 msec steps and model random variable PIR as a *discrete* random variable. We recall that notation $(PIR = k)$ denotes the event "the packet-inter reception time equals $k \cdot 100$ msec".

A. The geometric link model

The geometric model corresponds to the well-known model of independent Bernoulli trials, according to which each transmission is successfully received with a fixed probability p. Success probability p is assumed to be independent of the vehicles' speed and relative distance, as long as the two vehicles fall into each other transmission range. When the two vehicles are outside each other transmission range, the reception probability is assumed to be 0. This channel model has been used, e.g., in [13], [16].

It is straightforward to see that the geometric link model induces a PIR time distribution which is geometric of parameter p, whence the name of the model. In fact, we have

$$P(PIR = k) = (1-p)^{k-1}p \ ,$$

for $k = 1, 2, \ldots$.

It is also easy to see that the ccdf of the PIR time is:

$$P(PIR > k) = (1-p)^{k} \ .$$

A log-log plot of the PIR time ccdf with geometric link model and different values of p is reported in Figure 7. As seen from the plot, the tail of the PIR time distribution is very thin, unless parameter p is relatively low.

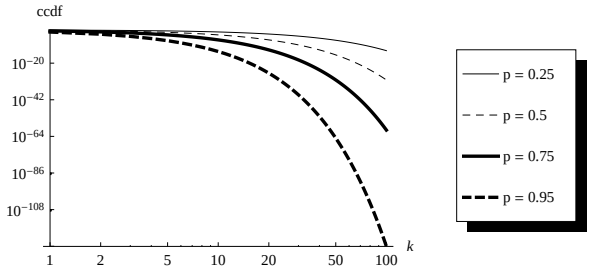

Fig. 7. Ccdf of the PIR time distribution with geometric link model and different values of parameter p.

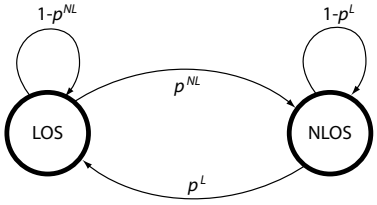

Fig. 8. The L/N link model.

B. The Gilbert model

The Gilbert model has been introduced in [8] to model bit error bursts in packet switched networks. In the Gilbert model, the link can be in two states (GOOD and BAD): when in GOOD state, the bit is correctly received with probability 1; when in BAD state, the bit is correctely received with probability $0 \leq p_{low} < 1$. Transitions between the two states are determined according to transition probabilities p_G and p_B. Thus, the model is fully characterized by three parameters: the link reception probability in BAD state p_{low}, and the two transition probabilities p_G and p_B.

The PIR time distribution in the Gilbert model can be obtained as a special case of that for the more general Gilbert-Elliot model derived in the next section. Similarly to the geometric link model, we assume the above packet reception probabilities apply only when the two vehicles are within each other transmission range, with reception probability equal to 0 otherwise.

C. The L/N (Gilbert-Elliot) link model

In [6], Elliot introduced a generalization of the Gilbert model in which the probability of correct bit reception in GOOD state is p_{high}, with $p_{low} < p_{high} \leq 1$. The resultant model is known as the Gilbert-Elliot model. In this paper, we propose to rename the Gilbert-Elliot model in vehicular environments as L/N link model, motivated by the observation that beacon reception probability is heavily influenced by LOS (corresponding to GOOD state) and NLOS (corresponding to BAD state) conditions. This observation has been recently confirmed by measurement studies [2]. The resulting 2×2 Markov chain is pictorially represented in Figure 8. A link can be in either LOS or NLOS state, with transition probabilities p^L, p^{NL} determining the rate of transitions between the two states. The probability of successfully receiving a packet depends on the current link state: it is p_{high}, with $0 < p_{high} < 1$, when the link is in LOS state, and it is p_{low}, with $0 < p_{low} < p_{high}$, when the link is in NLOS state. Note that, given the memorylessness property of a Markov chain, the probability of successfully receiving a beacon at time t depends only on the state of the link at time t, and not on its state at previous time steps. Similarly to the geometric and Gilbert model, we assume the above packet reception probabilities apply only when the two vehicles are within each other transmission range, with reception probability equal to 0 otherwise.

The Gilbert-Elliot model has been mostly used so far to characterize bit-level error burst in a communication, thus the typical quantity of interest has been the number of correctly received bits in a group of m consecutive bits. In this paper, we are instead interested in characterizing the distribution of two consecutive successful receptions (corresponding to packet, instead of bit, receptions), which, to our best knowledge, has not been studied so far.

To derive the PIR time distribution in the L/N-model, we start by stating a known property of the two states Markov chain defined above:

Proposition 1 (see, e.g., [3]): If $0 < p^L, p^{NL} < 1$, the unique stationary distribution of the two states Markov chain of Figure 8 is

$$\pi = \left(p_L = \frac{p^L}{p^L + p^{NL}}, \;\; p_{NL} = \frac{p^{NL}}{p^L + p^{NL}} \right) .$$

Thus, p_L and $p_{NL} = 1 - p_L$ represent the stationary probabilities of finding the link in state LOS and NLOS, respectively.

Next, we derive the probability $P(L|Rx)$ (respectively, $P(NL|Rx)$) of finding the link in state LOS (respectively, NLOS), conditioned on the event that a beacon has been received. Probability $P(L|Rx)$ can be computed applying Bayes' theorem, according to which we can write:

$$\begin{aligned} P(L|Rx) &= \frac{P(Rx|L) \cdot P(L)}{P(Rx)} = \frac{p_{high} \cdot p_L}{p_L \cdot p_{high} + p_{NL} \cdot p_{low}} = \\ &= \frac{p_{high} \cdot p^L}{p^L \cdot p_{high} + p^{NL} \cdot p_{low}} \end{aligned}$$

and

$$P(NL|Rx) = 1 - P(L|Rx) = \frac{p_{low} \cdot p^{NL}}{p^L \cdot p_{high} + p^{NL} \cdot p_{low}}$$

The value of $P(PIR = k)$, for any $k \geq 1$, can be computed by considering all possible unfolding of the Markov chain during k steps, starting from a reception event. Consider a given k-step unfolding of the Markov chain, i.e. a sequence of k states $S_1, \ldots, S_k$, with $S_i \in \{LOS, NLOS\}$, and let $P(S_1, \ldots, S_k)$ be the probability that the unfolding occurs. The probability that $(PIR = k)$ occurs, conditioned on unfolding $S_1, \ldots, S_k$, can be computed as follows:

$$P(PIR = k | \{S_1, \ldots, S_k\}) = p_{S_k} \cdot \prod_{i=1}^{k-1} (1 - p_{S_i}) \; ,$$

where $p_{S_i} = p_{high}$ if $S_i = LOS$, and $p_{S_i} = p_{low}$ if $S_i = NLOS$.

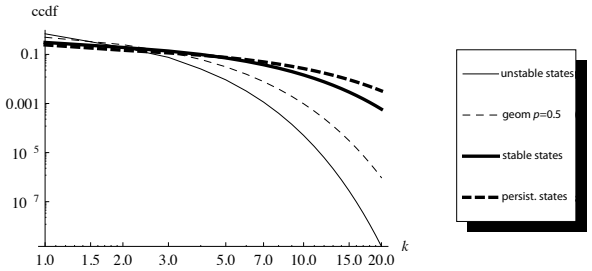

Fig. 9. Ccdf of the PIR time distribution with L/N link model and different parameter settings.

The probability that unfolding $S_1, \ldots, S_k$ occurs after a reception event can be computed as follows:

$$P(S_1, \ldots, S_k) = P(L|Rx) \cdot \prod_{i=1}^{k} p^{L,S_i} + P(NL|Rx) \cdot \prod_{i=1}^{k} p^{NL,S_i} \ ,$$

where

$$p^{L,S_1} = \begin{cases} 1 - p^{NL} & \text{if } S_1 = LOS \\ p^{NL} & \text{otherwise} \end{cases}$$

and

$$p^{L,S_i} = \begin{cases} 1 - p^{NL} & \text{if } S_{i-1} = LOS, \ S_i = LOS \\ p^{NL} & \text{if } S_{i-1} = LOS, \ S_i = NLOS \\ p^{L} & \text{if } S_{i-1} = NLOS, \ S_i = LOS \\ 1 - p^{L} & \text{if } S_{i-1} = NLOS, \ S_i = NLOS \end{cases}$$

for $i > 1$. The probabilities p^{NL,S_i} are defined similarly.

Thus, the probability of event $(PIR = k)$ can be computed as follows

$$P(PIR = k) = \sum p_{S_k} \cdot \prod_{i=1}^{k-1} (1 - p_{S_i}) \cdot P(S_1, \ldots, S_k) \ ,$$

where the summation is over all possible k-step unfolding of the Markov chain. Unfortunately, directly computing $P(PIR = k)$ requires summing a number of terms which is exponential in k, which becomes unfeasible for even moderate values of k. However, the $P(PIR = k)$ probabilities can be efficiently computed using the following recursive definition, whose correctness can be formally proved by induction (proof omitted due to lack of space):

$$P(PIR = k) = P(L|Rx) P_{kL} + P(NL|Rx) P_{kN} \ ,$$

where

$$P_{iL} = p^{NL}(1 - p_{low}) P_{(i-1)N} + (1 - p^{NL})(1 - p_{high}) P_{(i-1)L}$$

$$P_{iN} = (1 - p^{L})(1 - p_{low}) P_{(i-1)N} + p^{L}(1 - p_{high}) P_{(i-1)L}$$

for $i = 2, \ldots, k$ and

$$P_{1L} = (1 - p^{NL}) p_{high} + p^{NL} p_{low}$$

$$P_{1N} = (1 - p^{L}) p_{low} + p^{L} p_{high} \ .$$

The ccdf of the PIR time distribution with the L/N link model and different parameter settings is shown in Figure 9. In all the plots reported in the figure, $p_{high} = 0.9$, $p_{low} = 0.1$, and $p^L = p^{NL}$. With these settings, it is easy to see that the probability of successful reception is $p_L \cdot p_{high} + p_{NL} \cdot p_{low} = 0.5$. Different scenarios are considered, modeling a situation where transitions between LOS and NLOS states are relatively frequent ($p^L = p^{NL} = 0.8$ – *unstable* plot), relatively unfrequent ($p^L = p^{NL} = 0.2$ – *stable* plot), and seldom ($p^L = p^{NL} = 0.1$ – *persistent* plot). For comparison purposes, the plot corresponding to the geometric link model with $p = 0.5$ is also reported. As seen from Figure 9, with the L/N link model the shape of the ccdf varies considerably even if the probability of successful reception is fixed at 0.5. In particular, scenarios with relatively persistent link states result in a fatter tail of the PIR distribution.

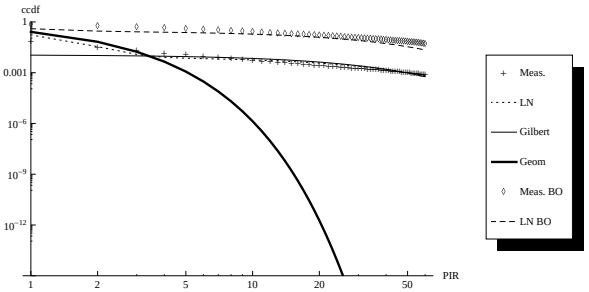

Fig. 10. Measurement-based PIR time ccdf and geometric, Gilbert, and L/N model fittings: unconditioned and conditioned distribution.

D. Validation

Can the link models defined above be used to faithfully mimic beacon reception behavior in vehicular networks? To answer this question, we have fitted the geometric, Gilbert and L/N link models to the data obtained from our traces.

Fitting of the geometric model has been done as follows. The expected value of random variable PIR under the geometric link model is $1/p$. Thus, the parameter p of the geometric link model for a specific data set (either strict or loose transmission range) can be computed by setting $p = 1/Avg(PIR)$, where $Avg(PIR)$ corresponds to the average PIR value observed in the experiments. The resulting values of p are 0.7918 and 0.7411 in the strict and loose transmission range case, respectively.

Fitting of the Gilbert and L/N link model is less straightforward, since the models have three and four parameters, respectively, and the expected value of random variable PIR in these models cannot be readily computed. We have then performed an iterative search for the best values of the model parameters, minimizing the mean square error (in log scale).

Figure 10 reports the ccdf of the PIR time distribution derived from measurements, as well as the geometric, Gilbert and L/N model fits in case of loose transmission range. Similar results, not reported due to lack of space, have been obtained in case of strict transmission range. From the figure is seen that the geometric link model generates a packet reception behavior that deviates considerably from measured data. The Gilbert model shows a better fit to measurements than the geometric model: however, while it can be used to approximate reasonably well the tail of the distribution, it is quite inaccurate in estimating the first terms of the distribution. The L/N model can be instead be adjusted to almost perfectly fit

experimental data. The resulting best fitting for the L/N model are $p^L = 0.035, p^{NL} = 0.004, p_{high} = 0.825, p_{low} = 0.0125$ in the strict transmission range case, and $p^L = 0.03, p^{NL} = 0.005, p_{high} = 0.835, p_{low} = 0.0125$ in the loose transmission range case. It is interesting to observe that the two best fittings of the L/N model are indeed very similar, indicating that the optimal setting of this model is not very much dependent on the choice of the transmission range.

To further validate accuracy of the L/N-model, we have considered the conditional PIR time distribution after a blackout event, as defined in Section V. The conditional PIR time distribution for the L/N-model has been has been evaluated by simulating the Markov chain with best fit parameters for 10^6 steps, and recording the observed PIR time after a blackout event. The resulting conditional PIR time distribution is reported in Figure 10, along with that obtained from measurements. As seen from the figure, the L/N-model with best fit parameters as above is able to faithfully reproduce both the unconditioned and conditioned PIR time distribution obtained from measurements. On one hand, this *validates the L/N-model as a simple, analytically tractable, and very accurate vehicular link model*. On the other hand, the fact that L/N-model can be made to almost perfectly fit measured PIR time distribution indirectly proves that *the heavily tailed shape of the PIR time distribution is caused by transition between persistent LOS and NLOS conditions, during which reception probability is relatively high and relatively low, respectively*.

VIII. Final Remarks

In this paper, we have presented a first extensive, measurement-based analysis of beaconing performance in vehicular networks considering not only delivery rate, but also temporal beacon reception patterns. The major findings concerning temporal correlation of successful beacon receptions is that the PIR time distribution is heavily tailed, and that situation awareness blackouts are likely to occur in batch. As we have discussed in this paper, these findings have important implications on the design of active safety applications, challenging the design of effective solutions.

Another major contribution of this paper is an empirical proof of the fact that the observed beacon reception patterns are caused by transition between persistent LOS and NLOS link conditions; a byproduct of this proof is the validation of the L/N-model as a simple, analytically tractable, and very accurate vehicular link model, which we believe will be an invaluable tool to assist active safety application designers in the challenge of developing effective solutions.

Before ending this paper, an observation is in order. The fact that situation awareness blackouts are likely to occur in NLOS conditions apparently impairs the ultimate design goal of active safety applications, namely extending a driver's situation awareness *beyond human eye*. Our study clearly indicates that countermeasures should be undertaken to fulfill this goal. For instance, advanced PHY layer techniques (multi-antenna systems, advanced coding schemes allowing reception of a beacon even if only a few bits are corrupted, etc.) could be used to increase reception probability in NLOS conditions. A network-level countermeasure is multi-hop propagation of beacons, so that impairment of the LOS path can be somehow avoided. However, usage of multi-hop communication can be considered as an effective approach only when the penetration rate of DSRC-based radio technology will be very high. Thus, how to increase reception probability in presence of NLOS conditions is likely to remain a prominent engineering challenge for several years to come.

References

[1] F. Bai, D.D. Stancil, H. Krishnan, "Toward Understanding Characteristics of Dedicated Short Range Communications (DSRC) From a Perspective of Vehicular Network Engineers", *Proc. ACM Mobicom*, pp. 329–340, 2010.

[2] M Boban, T.T.V. Vinhoza, M. Ferreira, J. Barros, O.K. Tonguz, "Impact of Vehicles as Obstacles in Vehicular Ad Hoc Networks", *IEEE J. Selected Areas in Communications*, Vol. 29, n. 1, pp. 15–28, Jan. 2011.

[3] A.E.F. Clementi, C. Macci, A. Monti, F. Pasquale, R. Silvestri, "Flooding Time of Edge-Markovian Evolving Graphs", *SIAM Journal of Discrete Mathematics*, Vol. 24, n. 4, pp. 1694–1712, 2010.

[4] "Standard Specification for Telecommunications and Information Exchange Between Roadside and Vehicle Systems - 5Ghz Band Dedicated Short Range Communications (DSRC)", *ASTM E2212-03*, 2003.

[5] T. ElBatt, S.K. Goel, G. Holland, H. Krishnan, J. Parikh, "Cooperative Collision Warning Using Dedicated Short Range Wireless Communications", *Proc. ACM VANET*, pp. 1–9, 2006.

[6] E.O. Elliot, "Estimates of Error Rates for Codes on Burst-Noise Channels", *Bell Syst. Tech. J.*, Vol. 42, pp. 1977–1997, 1963.

[7] ETSI TC ITS, "Intelligent Transportation Systems (ITS): European Profile Standard on the Physical and Medium Access Layer of 5Ghz ITSs", draft ETSI ES 202 663 V.0.0.6, Oct. 2009.

[8] E.N. Gilbert, "Capacity of Burst-Noise Channel", *Bell Syst. Tech. J.*, Vol. 39, pp, 1253–1265, 1960.

[9] K. Hong, D. Xing, V. Rai, J. Kenney, "Characterization of DSRC Performance as a Function of Transmit Power", *Proc. ACM VANET*, pp. 63–68, 2009.

[10] D. Jiang, Q. Chen, L. Delgrossi, "Optimal Data Rate Selection for Vehicle Safety Communications", *Proc. ACM VANET*, pp. 30–38, 2008.

[11] J.B. Kenney, "Standards and Regulations", in *VANET: Vehicular Applications and Inter-Networking Technologies*, John Wiley and Sons, Chichester, UK, 2009.

[12] A. Paier, R. Tresch, A. Alonso, D. Smely, P. Meckel, Y. Zhou, N. Czink, "Average Downstream Performance of Measured IEEE 802.11p Infrastructure-to-Vehicle Links", *Proc. Workshop on Vehicular Connectivity*, 2010.

[13] G. Resta, P. Santi, J. Simon, "Analysis of Multi-Hop Emergency Message Propagation in Vehicular Ad Hoc Networks", *Proc. ACM MobiHoc*, pp. 140-149, 2007.

[14] M. Torrent-Moreno, D. Jiang, H. Hartenstein, "Broadcast Reception Rates and Effects of Priority Access in 802.11-based Vehicular Ad Hoc Networks", *Proc. ACM VANET*, pp. 11–18, 2004.

[15] VSC Consortium, "Vehicle Safety Communications Project Task 3 – Final Report: Indentify Intelligent Vehicle Safety Applications Enables by DSRC, *DOT HS 809 859*, March 2005.

[16] X. Yang, J. Liu, F. Zhao, N.H. Vaidya, "A Vehicle-to-Vehicle Communication Protocol for Cooperative Collision Warning", *Proc. IEEE MobiQuitous*, pp. 1–10, 2004.